JCTC Journal of Chemical Theory and Computation

Article

pubs.acs.org/JCTC

Benchmark Calculations of Three-Body Intermolecular Interactions and the Performance of Low-Cost Electronic Structure Methods

Jan Řezáč,[†] Yuanhang Huang,[‡] Pavel Hobza,[†,§] and Gregory J. O. Beran*[,‡]

[†]Institute of Organic Chemistry and Biochemistry, Academy of Sciences of the Czech Republic, 166 10 Prague, Czech Republic

[‡]Department of Chemistry, University of California, Riverside, California 92521 United States

[§]Regional Centre of Advanced Technologies and Materials, Department of Physical Chemistry, Palacký University, 771 46 Olomouc, Czech Republic

Supporting Information

ABSTRACT: Many-body noncovalent interactions are increasingly important in large and/or condensed-phase systems, but the current understanding of how well various models predict these interactions is limited. Here, benchmark complete-basis set coupled cluster singles, doubles, and perturbative triples (CCSD(T)) calculations have been performed to generate a new test set for three-body intermolecular interactions. This "3B-69" benchmark set includes three-body interaction energies for 69 total trimer structures, consisting of three structures from each of 23 different molecular crystals. By including structures that exhibit a variety of intermolecular interactions and packing arrangements, this set provides a stringent test for the ability of electronic structure methods to describe the correct physics involved in the interactions. Both MP2.5 (the average of second- and third-order Møller−Plesset perturbation theory) and spin-component-scaled CCSD for noncovalent interactions (SCS-MI-CCSD) perform well. MP2 handles the polarization aspects reasonably well, but it omits three-body dispersion. In contrast, many widely used density functionals corrected with three-body D3 dispersion correction perform comparatively poorly. The primary difficulty stems from the treatment of exchange and polarization in the functionals rather than from the dispersion correction, though the three-body dispersion may also be moderately underestimated by the D3 correction.

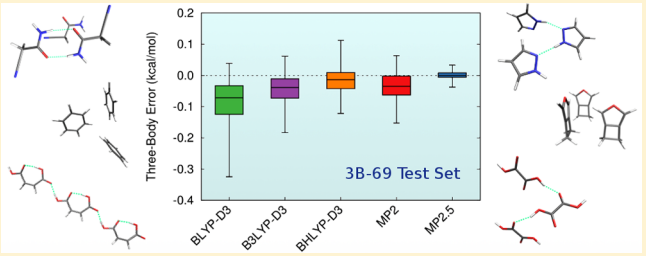

1. INTRODUCTION

Noncovalent interactions play a critical role in the behavior of molecular liquids, solids, and supramolecular systems. The strongest noncovalent intermolecular interactions typically occur between pairs of molecules/functional groups. Nonadditive intermolecular interactions between larger sets of molecules can also be important, however. While individual three-body and higher interactions are often weaker than their two-body counterparts, summing these small many-body contributions over the large numbers of proximal trimers, tetramers, and larger clusters in a condensed-phase system can generate a substantial net energy contribution. Intermolecular many-body interactions often account for 10−20% of the lattice energy of a molecular crystal, for instance.[1] Many-body interactions are equally important within a single, large molecule—consider the noncovalent interactions between residues in a protein, for instance.

The role of polarization and cooperative hydrogen bonding in producing these many-body interactions is well-known. In water clusters, for instance, the many-body contribution arising from hydrogen bond cooperativity can contribute 30% or more to the total cluster binding energy.[2] However, research over the past few years has demonstrated that many-body London dispersion contributions may play an important role in understanding the molecular condensed phase.[3−15] In crystalline benzene, the many-body contribution, which is dominated by dispersion, contributes ∼10% to the overall lattice energy.[3,5,16,17] Likewise, adding (interatomic) many-body dispersion to the X23 test set of molecular crystal lattice energies reduces the errors by a factor of 2.[8]

Given the chemical significance of noncovalent interactions, it is important to develop or identify electronic structure methods capable of describing these interactions with reasonable computational effort. The advent of benchmark test sets like S22,[18,19] S66,[20,21] X40,[22] 1HSG,[23] S12L,[13] and others for dimer noncovalent interactions has provided an important means of validating and comparing different methods. No such comprehensive test set currently exists for many-body interactions, however. High-quality benchmark calculations for the many-body terms in selected systems such as benzene crystal have been reported,[16,17] but demonstrating the reliability of a method requires tests on larger numbers of more chemically diverse systems. The related C21[24] and X23[8] test sets provide valuable reference experimental lattice/sublimation energies for molecular crystals.

Received: March 24, 2015

DOI: 10.1021/acs.jctc.5b00281
J. Chem. Theory Comput. XXXX, XXX, XXX−XXX

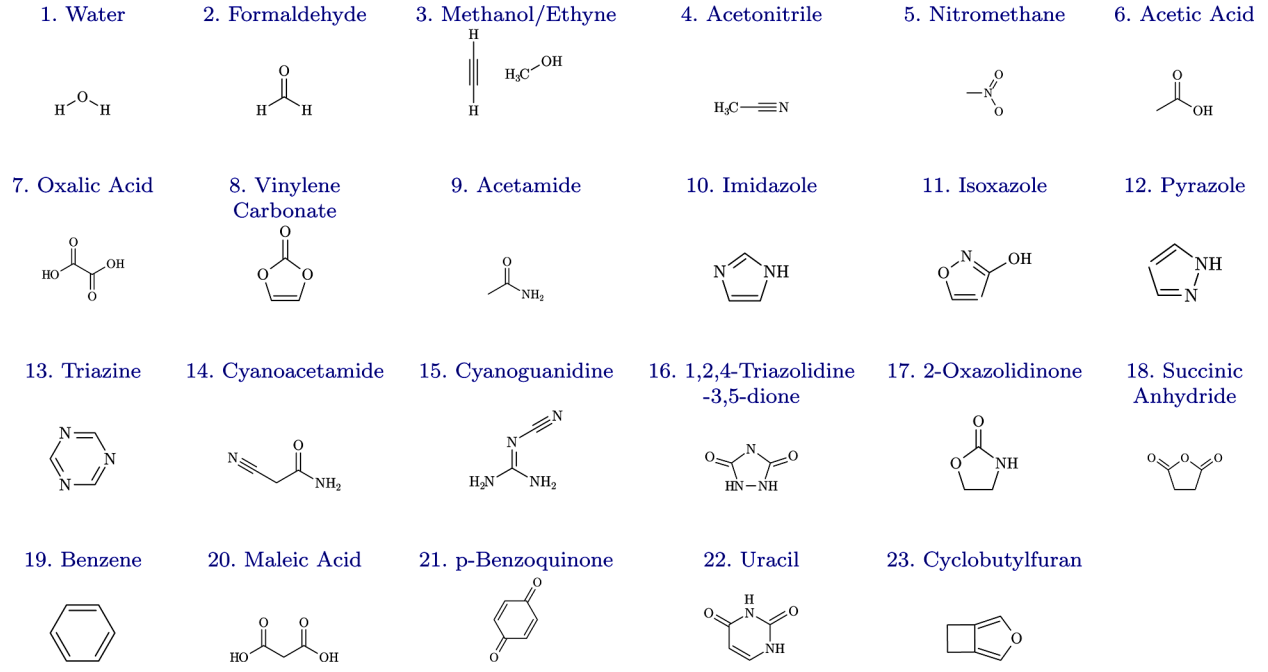

Figure 1. 3B-69 test set contains trimers of 23 species with three different geometric arrangements each, for a total of 69 structures.

Still, one often desires high-level electronic structure reference values to compare against to avoid the complexities and approximations introduced when benchmarking against experiment. In addition, knowing how electronic structure methods perform for these noncovalent many-body interactions also provides insights into their behavior in large molecules for which benchmark calculations are not tractable. Indeed, many dispersion-corrected density functional methods perform well in small benchmark dimers, but how this performance translates to larger systems remains an open question that has been the subject of recent research[13,25,26] and which would benefit from additional high-accuracy benchmarks.

This work presents a "3B-69" benchmark test set for three-body intermolecular interactions in 69 trimers of organic molecules containing carbon, hydrogen, oxygen, and nitrogen that will allow validation and comparison of methods for many-body interactions. Three-body contributions are typically the largest many-body interactions, but higher-order terms can also be important.[17,27] At the same time, benchmark electronic structure calculations on larger clusters of molecules quickly become computationally infeasible, so the current set does not go beyond trimers.

Several considerations were taken into account when designing the 3B-69 test set. A useful many-body interaction benchmark suite should include clusters with a mixture of many-body polarization and dispersion interactions. The polarization contribution is largely governed by the polarity of the molecules and the potential for cooperative hydrogen bonding effects, which of course depends on the geometric arrangement. The dispersion contribution generally increases with molecular size, and it is typically largest in systems with highly polarizable electron densities (e.g., extended π-electron systems). Because the leading Axilrod–Teller–Muto (ATM) three-body dispersion contribution[28,29] scales as R^{-9}, many-body dispersion energies are strongly affected by the packing density. In the oxalyl dihydrazide crystal, for example, the importance of three-body intermolecular dispersion in determining relative polymorph stability stems primarily from the significantly higher packing density of the α polymorph relative to the other four polymorphs.[4]

The new 3B-69 benchmark set presented here consists of three trimer geometries extracted from each of 23 different molecular crystals, for 69 total trimers. Extracting the trimers from molecular crystals ensures chemically realistic geometries. Varying both the chemical species and geometric packing provides control over the proportions and magnitudes of the polarization and dispersion contributions. The chemical species include nonpolar species like benzene and triazine, polar species like nitromethane and succinic anhydride, and hydrogen-bonded species such as maleic acid and water. The test species contain up to eight non-hydrogen atoms per molecule, thereby ensuring the feasibility of benchmark coupled cluster singles and doubles plus perturbative triples (CCSD(T)) calculations on the trimers. This constraint on the maximum molecular size does limit the overall magnitude of the many-body dispersion energies, but the variety of structures included in the test set should ensure that methods that perform uniformly well across the different systems correctly describe the underlying physics of the many-body noncovalent interactions.

The following sections describe the composition of the test set and how the structures and benchmark CCSD(T) three-body energies were obtained. In addition, the performance of several other methods for computing the three-body interactions are tested. Second-order Møller–Plesset perturbation theory (MP2) captures many-body polarization effects, but three-body and higher dispersion terms do not appear until at least third order (MP3).[30] Other methods like spin-component-scaled coupled cluster singles and doubles (CCSD) models[31,32] and MP2.5[33,34] describe three-body effects as accurately as two-body interaction energies. Density functional theory with dispersion correction including a three-body contribution is tested as well.

DOI: 10.1021/acs.jctc.5b00281
J. Chem. Theory Comput. XXXX, XXX, XXX–XXX

2. COMPUTATIONAL METHODS

2.1. Composition of the Data Set. The test set consists of 69 total trimer structures, with three trimers extracted from each of 23 molecular crystals. In several cases, the trimers were extracted from multiple different crystal polymorphs. Most crystal structures were taken from the Cambridge Structure Database hosted by the Cambridge Crystallographic Data Center (CCDC). CCDC reference codes or other literature references for the experimental structures are provided in parentheses below.

The chemical species were chosen to represent a variety of intermolecular interactions and intermolecular packing motifs. The set includes (Figure 1) the following: acetamide (ACEMID05), acetic acid (ACETAC07, ACETAC09), acetonitrile (QQQCIV01, QQQCIV04), benzene (BENZEN14), cyanoacetamide (CYANAC), cyanoguanidine (CYAMPD03), cyclobutylfuran (XULDUD, XULDUD01), formaldehyde (KEMZIL01), imidazole (IMAZOL06), isoxazole (NEZMUA), maleic acid (MALIAC12, MALIAC13), methanol/ethyne (CIYYEP), nitromethane (NTROMA15), oxalic acid (OXALAC04, OXALAC06), 2-oxazolidinone (OXAZIL01), parabenzoquinone (BNZQUI03), pyrazole (PYRZOL05), succinic anhydride (SUCANH16), triazine (TRIZIN03), 1,2,4-triazolidine-3,5-dione (KOXRIY), uracil (URACIL), vinylene carbonate (VINYLC), and water (ice Ih[35] and a triangular geometry).

2.2. Geometry Optimizations. The experimental crystal structures were relaxed using B3-LYP-D*, which combines B3-LYP[36] with the empirical two-body dispersion correction of Civalleri and co-workers,[37] and the TZP basis[38] using Crystal 09.[39] The crystal lattice parameters were held fixed at their experimental values during the optimizations. The agreement between the optimized and experimental structures is good, with an average rmsd15[40] of 0.07 Å (maximum 0.16 Å) for non-hydrogen atoms. The final trimer geometries were extracted from the optimized crystal structures. For water, two of the three geometries were extracted from the structure of ice Ih. The third water cluster is an optimized gas-phase trimer in a triangular geometry. Images and Cartesian coordinates for all 69 trimer structures are provided as Supporting Information.

2.3. Three-Body Energies. The three-body energies ΔE^3 studied in this work are defined as a difference between the total energy of the trimer and a sum of both monomer energies and all two-body interaction energies ΔE^2 between them. For a trimer consisting of units *A*, *B*, and *C*, the three-body energy is

$$\Delta E^3(ABC) = E(ABC) - E(A) - E(B) - E(C) - \Delta E^2(AB) - \Delta E^2(BC) - \Delta E^2(CA) \quad (1)$$

Expanding the interaction energies in terms of monomer and dimer energies, e.g. $\Delta E^2(AB) = E(AB) - E(A) - E(B)$, the three-body energy can be expressed in terms of monomer, dimer, and trimer energies as

$$\Delta E^3(ABC) = E(ABC) - E(AB) - E(BC) - E(CA) + E(A) + E(B) + E(C) \quad (2)$$

To eliminate the basis set superposition error (BSSE) in trimer calculations, an appropriate counterpoise correction should be used. There are multiple ways how to define BSSE correction in a three-body system when the total energy is calculated.[2] However, when a three-body contribution ΔE^3 is sought, the most satisfactory approach is to perform the monomer and dimer calculations in the trimer basis.[41] This scheme is computationally demanding because it requires seven calculations in the trimer basis for each structure.

Counterpoise correction is a controversial topic, and some authors recommend not using it at all.[42,43] However, in 2-body interactions, both formal analysis[44] and numerical evidence including recent, very accurate calculations[45] clearly prove its benefits. In many-body expansions, counterpoise correction is also important.[2,46,47] In our calculations, there are two reasons for using it. First, the CCSD(T) correction is calculated in a relatively small aug-cc-pVDZ basis set where basis set superposition cannot be neglected. Second, it had been shown that the counterpoise correction improves the convergence of CBS extrapolation we apply to the MP2 correlation energy. Accordingly, employing a counterpoise correction in this work very probably improves the benchmark CCSD(T) results. For consistency, we also employ counterpoise correction in all other wave function methods used here. This allows one-to-one comparison of the results where possible artifacts of the correction are likely to cancel. We do not employ it in the DFT calculations, however, since the BSSE is less significant than in correlated calculations.

To calculate the three-body energies efficiently, the procedure was automated using the Cuby framework[48] developed by one of the authors (J.Ř.). Cuby handles the extraction of the monomers from the trimer, preparation of the inputs for any interfaced software package, and processing the results.

2.4. Benchmark Calculations. The benchmark three-body energies are calculated using the composite CCSD(T)/CBS approach.[49,50] Correlation consistent basis sets[51] augmented with diffuse functions[52] are used; in the following text, we abbreviate the basis set names aug-cc-pVXZ (X = D, T, Q) as aXZ. The composite CCSD(T)/CBS result is constructed from three contributions: the Hartree−Fock energy E^{HF}, the MP2 correlation energy E^{MP2}, and the correction term $\Delta\mathrm{CCSD(T)} = E^{CCSD(T)} - E^{MP2}$. The Hartree−Fock energy is calculated in the aQZ basis. The MP2 correlation energy is extrapolated[53] to CBS limit from the aTZ and aQZ basis sets. Finally, the ΔCCSD(T) correction is calculated in the aDZ basis. The ΔCCSD(T)/aDZ correction was validated in the aTZ basis for the dozen smallest trimers in the set. The same approach was used to generate earlier benchmark data sets of interaction energies,[22,54,55] and the accuracy of this scheme with the CCSD(T) correction calculated in the aDZ basis set with respect to converged CCSD(T)/CBS results[56] was estimated to be about 2%.

To evaluate the importance of the three-body effects in the studied systems, we also calculated the 2-body (interaction) energies among all possible pairs of dimers in each trimer at the same level of theory. The standard counterpoise correction[57] was employed for the two-body calculations.

These benchmark calculations were performed using Turbomole 6.5.[58] The resolution of identity approximation (RI) was employed in the MP2 calculations.[59]

2.5. Force Field Energy Decomposition of the Interaction Energies. To help interpret the benchmark results presented below, we will assess the nature of the three-body intermolecular interactions in each trimer. Kohn−Sham-based symmetry-adapted perturbation theory (SAPT(DFT))[60] could provide a natural framework for classifying intermolecular interactions, but three-body SAPT(DFT) calculations are

DOI: 10.1021/acs.jctc.5b00281
J. Chem. Theory Comput. XXXX, XXX, XXX−XXX

computationally demanding. Instead, we utilize a simpler *ab initio* force field (AIFF)[3,61] based on asymptotic intermolecular perturbation theory (with short-range empirical damping) to characterize the three-body intermolecular interactions in each trimer geometry.

The three-body AIFF contribution examined here includes self-consistent polarization and ATM three-body dispersion. The force field is parametrized with atom-centered distributed multipoles, distributed polarizabilities, and dispersion coefficients which are calculated from (time-dependent) density functional theory using asymptotically corrected PBE0 and the Sadlej basis set.[62,63] Empirical short-range damping is applied to both the polarization and three-body dispersion using Tang-Toennies damping functions, as described previously.[3,61]

It is an oversimplification to attribute the three-body intermolecular interactions to polarization and dispersion only. The three-body SAPT(DFT) expansion includes a variety of exchange and other additional terms[60] beyond polarization and dispersion. The empirical damping functions employed in the force field do compensate somewhat for the lack of exchange terms. However, the polarization contribution can be especially sensitive to the short-range damping, and the optimal damping parameters can vary from system to system. Previous experience suggests that values between $\beta = 1.3-1.45$ Bohr are often optimal for organic molecules.[3,4,61,64] Here, an induction damping parameter of $\beta = 1.4$ Bohr was used, with no attempt to optimize β for individual systems. The three-body dispersion was damped using a damping function described previously and representative van der Waals radii of 2.63, 3.34, 3.18, and 3.07 Bohr for hydrogen, carbon, nitrogen, and oxygen, respectively.[65] No attempt was made to optimize these damping function parameters here.

The three-body force field polarization and ATM dispersion contributions used here have performed well in previous studies.[3,4,61,64] In the Results section below, we will demonstrate that the force field dispersion and polarization contributions do behave in expected ways and correlate well with the results obtained from the electronic structure methods, making them a useful semiquantitative tool for analyzing the three-body interactions.

2.6. Tested Wave Function Methods. In addition to performing the benchmark CCSD(T) calculations, we examine the accuracy of several less-expensive correlated wave function methods. In all methods beyond MP2, the CBS limit is estimated using a scheme analogous to the benchmark calculations, in which a higher-order correction calculated in the aDZ basis set is added to the MP2/CBS result obtained as described above.

The first set of methods is based on CCSD. In addition to conventional CCSD, we also tested its spin component scaled variant SCS-CCSD[31] and its modification optimized for noncovalent interactions, SCS-MI-CCSD.[32] The next step down in the computational demands is MP3 and its scaled variant, MP2.5.[33] MP2.5 empirically scales the MP3 term in the perturbation theory series by a factor of 0.5, which means the correlation energy is an average of MP2 and MP3 results. Despite its empiricism, MP2.5 systematically improves interaction energies in a wide range of noncovalent complexes.[34]

The MP3 calculations were performed in Turbomole 6.5[58] using the RI approximation. At the CCSD level, we used the frozen natural orbital (FNO) approximation[66,67] available in the PSI4 package,[68] which makes the calculations considerably more efficient (especially when ghost basis functions are present). Test calculations on the 11 smallest trimers demonstrated that the differences between FNO-CCSD and conventional CCSD were negligible (average difference 0.001 kcal/mol, maximum 0.003 kcal/mol).

2.7. Tested DFT Methods. A variety of widely used density functionals were also tested on these systems, including B-LYP, B3-LYP, BH-LYP, CAM-B3-LYP, PBE, PBE0, TPSS, M06-2X, M06-HF, and B2-PLYP. Three-body dispersion was incorporated using Grimme's D3 dispersion correction.[11]

The D3 dispersion correction contains a three-body term based on a damped ATM formula,[28,29] the necessary C_9^{ABC} coefficients are estimated from the two-body C_6 coefficients which are available for all atomic pairs. In turn, these C_6 coefficients were obtained via Casimir-Polder integration over atom-centered frequency-dependent dipole polarizabilities which were computed on reference hydrides using time-dependent DFT.

Note that the two-body D3 correction exists in two variants, the original one using a damping function that approaches zero at short distances (zero damping), and the Becke-Johnson damping introduced later,[69] but both versions use the same three-body term with zero damping. The damping function contains two parameters: an exponent α that determines the sharpness of the damping and a scaling factor for radii s_r used to adjust the threshold distance. Unless noted otherwise, we use the default values of $\alpha = 16$ and $s_r = 1.33$ which were defined in the original work as independent of the functional used.

Furthermore, the two-body part of the D3 correction is not exactly pairwise additive because each atomic C_6 coefficient is a function of the geometry of the whole system. As a result, the C_6 coefficients differ slightly in dimer and trimer. However, this effect is negligibly small, and, because it has no physical justification, we do not consider it in our calculations.

The CAM-B3-LYP functional calculations were carried out in ORCA version 3.0.[70] The M06-2X and M06-HF results were obtained with Molpro 2012.1[71,72] using the RI approximation. The remaining DFT calculations were performed in Turbomole 6.5[58] using the RI approximation.

3. RESULTS AND DISCUSSION

3.1. Benchmark Three-Body Energies. First, we explore the convergence of the three-body energies with basis set size. The benchmark CCSD(T)/CBS results are obtained as a composite of MP2/CBS results plus a smaller basis ΔCCSD-(T) correction. For the four smallest sets of trimers (water, formaldehyde, methanol/ethyne, and acetonitrile), we evaluated the ΔCCSD(T) correction in both aDZ and aTZ basis sets. The resulting CCSD(T)/CBS values differ only negligibly, with an RMSE of only 0.002 kcal/mol. For comparison, the average magnitude of the ΔCCSD(T) correction in this subset is 0.02 kcal/mol, while the average magnitude of the total three-body energy is 0.62 kcal/mol over the same subset. In other words, the three-body ΔCCSD(T) term is insensitive to the basis set size, and the composite three-body energies based on the CCSD(T)/aDZ calculations can be used safely in benchmarks. Because the CCSD(T) calculations in the aTZ basis set would be intractable for the vast majority of the data set, we use the ΔCCSD(T) correction computed in the aDZ basis for all the systems described in the remainder of the paper, including the four sets of systems for which the aTZ calculations are available.

DOI: 10.1021/acs.jctc.5b00281
J. Chem. Theory Comput. XXXX, XXX, XXX−XXX

Table 1. Composition of the Data Set, Estimated Contribution of London Dispersion, Group (Low/Medium/High Dispersion) and HF/aug-cc-pVQZ, MP2/CBS, and CCSD(T)/CBS Three-Body Energies (in kcal/mol)

number		system	dispersion (%)	group	HF	MP2/CBS	CCSD(T)/CBS
1	a	water	0.2	L	−1.396	−1.392	−1.386
	b	water	0.5	L	0.986	1.068	1.084
	c	water	1.5	L	−2.477	−2.472	−2.416
2	a	formaldehyde	0.8	L	−0.236	−0.168	−0.178
	b	formaldehyde	9.9	M	0.176	0.161	0.181
	c	formaldehyde	12.5	M	−0.136	−0.095	−0.093
3	a	methanol/ethyne	1.5	L	−1.265	−1.305	−1.308
	b	methanol/ethyne	30.8	H	0.030	0.036	0.047
	c	methanol/ethyne	16.4	M	−0.021	−0.003	0.023
4	a	acetonitrile	18.1	M	0.200	0.198	0.254
	b	acetonitrile	5.4	L	0.316	0.319	0.335
	c	acetonitrile	2.1	L	−0.177	−0.155	−0.166
5	a	nitromethane	16.3	M	−0.251	−0.178	−0.122
	b	nitromethane	21.2	M	0.241	0.216	0.255
	c	nitromethane	3.3	L	0.296	0.216	0.220
6	a	acetic acid	5.0	L	0.584	0.523	0.542
	b	acetic acid	0.8	L	−0.816	−0.937	−0.922
	c	acetic acid	26.0	H	−0.441	−0.248	−0.206
7	a	oxalic acid	15.9	M	−0.377	−0.267	−0.218
	b	oxalic acid	0.7	L	−1.137	−1.199	−1.198
	c	oxalic acid	3.1	L	−0.817	−0.791	−0.777
8	a	vinylene carbonate	0.9	L	−0.328	−0.310	−0.312
	b	vinylene carbonate	17.8	M	−0.265	−0.202	−0.147
	c	vinylene carbonate	5.3	L	−0.572	−0.521	−0.490
9	a	acetamide	73.7	H	−0.197	−0.239	−0.089
	b	acetamide	3.7	L	0.519	0.529	0.579
	c	acetamide	0.5	L	−0.862	−0.850	−0.860
10	a	imidazole	8.3	M	−0.785	−0.771	−0.663
	b	imidazole	22.0	M	0.255	0.208	0.270
	c	imidazole	0.3	L	−1.535	−1.631	−1.636
11	a	isoxazole	77.7	H	−0.065	0.083	0.176
	b	isoxazole	16.2	M	0.106	0.147	0.190
	c	isoxazole	4.6	L	−0.134	−0.105	−0.129
12	a	pyrazole	4.3	L	−1.408	−1.315	−1.283
	b	pyrazole	85.7	H	−0.062	0.010	0.067
	c	pyrazole	0.8	L	−0.334	−0.287	−0.293
13	a	triazine	88.1	H	−0.019	0.013	−0.005
	b	triazine	52.4	H	0.092	0.086	0.137
	c	triazine	48.8	H	0.026	0.052	0.125
14	a	cyanoacetamide	8.1	M	1.404	1.307	1.459
	b	cyanoacetamide	35.7	H	0.264	0.269	0.353
	c	cyanoacetamide	0.8	L	−1.367	−1.165	−1.228
15	a	cyanoguanidine	4.8	L	−1.027	−1.016	−0.907
	b	cyanoguanidine	31.9	H	0.333	0.474	0.577
	c	cyanoguanidine	16.4	M	0.136	0.089	0.138
16	a	triazolidinedione	20.0	M	−0.155	−0.126	−0.136
	b	triazolidinedione	5.3	L	0.699	0.681	0.780
	c	triazolidinedione	15.2	M	0.286	0.419	0.512
17	a	oxazolidinone	4.7	L	0.506	0.511	0.539
	b	oxazolidinone	15.9	M	−0.344	−0.315	−0.214
	c	oxazolidinone	0.2	L	0.143	0.145	0.154
18	a	succinic anhydride	12.1	M	0.454	0.380	0.432
	b	succinic anhydride	63.7	H	0.001	0.003	−0.001
	c	succinic anhydride	8.7	M	−0.153	−0.124	−0.131
19	a	benzene	57.3	H	−0.109	−0.054	0.048
	b	benzene	50.2	H	0.076	0.083	0.150
	c	benzene	40.3	H	−0.101	−0.061	−0.027
20	a	maleic acid	3.3	L	1.561	1.636	1.694
	b	maleic acid	0.1	L	−1.411	−1.428	−1.449
	c	maleic acid	10.2	M	−0.423	−0.347	−0.362

DOI: 10.1021/acs.jctc.5b00281
J. Chem. Theory Comput. XXXX, XXX, XXX−XXX

Table 1. continued

number		system	dispersion (%)	group	HF	MP2/CBS	CCSD(T)/CBS
21	a	p-benzoquinone	37.6	H	0.182	0.239	0.332
	b	p-benzoquinone	27.5	H	−0.042	−0.038	0.004
	c	p-benzoquinone	69.4	H	0.041	0.039	0.096
22	a	uracil	65.8	H	−0.042	−0.033	−0.004
	b	uracil	15.4	M	−0.334	−0.233	−0.238
	c	uracil	11.4	M	0.045	0.012	0.018
23	a	cyclobutylfuran	68.1	H	−0.165	−0.049	0.081
	b	cyclobutylfuran	54.2	H	0.049	0.071	0.138
	c	cyclobutylfuran	57.2	H	0.042	0.071	0.154

The benchmark CCSD(T)/CBS three-body energies for the entire data set are listed in Table 1. These data along with the geometries and results of selected tested methods are also available online in the BEGDB database.[73,74]

The average magnitude (absolute value) of the three-body energies is 0.46 kcal/mol. The strongest three-body contribution in the set, −2.42 kcal/mol, is found for a water trimer 1c (the negative sign indicates stabilization of the trimer due to the three-body effects). The largest destabilizing ΔE^3 of 1.69 kcal/mol was found in maleic acid trimer 20a. Overall, half of the trimers (34 out of 69 systems) exhibit stabilizing (negative) three-body energies. However, the structures with stabilizing three-body energies tend to exhibit stronger three-body energies than those with destabilizing three-body energies, and the average of the ΔE^3 energies is −0.11 kcal/mol.

To quantify the relative importance of the three-body effects in the studied systems, we also calculated all the pairwise interaction energies in the trimers at the same benchmark level. This allows us to express the ratio of the three-body energy with respect to the total stabilization energy of the trimer:

$$\Delta E^3_{rel}(ABC) = \frac{\Delta E^3(ABC)}{\Delta E^2(AB) + \Delta E^2(BC) + \Delta E^2(CA) + \Delta E^3(ABC)} \times 100\% \quad (3)$$

The average magnitude (absolute value) of ΔE^3_{rel} in the set is 4.0%, the largest contribution of three-body effects was found in water trimer 1b and amounts to −18.4%. The CCSD(T) interaction energies as well as the values of $\Delta E^3_{rel}(ABC)$ for the individual systems are available in Table S1 in the Supporting Information.

3.2. Characterization of the Test Set. Before discussing the performance of other electronic structure models on the benchmark set, we examine the nature of the intermolecular interactions in the different trimer geometries. Figure 2a plots the force-field-estimated three-body polarization and dispersion contributions for the different trimers. Two features stand out. First, typical polarization energies in these systems are ±0.5 kcal/mol, though many exceed that range. For example, the three-body polarization energies approach 2 kcal/mol in water trimer 1c and imidazole 10c trimer geometries. In contrast, the three-body dispersion interactions span a smaller range of ∼0.2 kcal/mol. The smaller magnitude of the dispersion energies is unsurprising given the relatively small size of the molecules in the test set.

Second, by design, the signs and magnitudes of the polarization and dispersion contributions vary significantly across the three different geometries for a given trimer. For example, acetamide trimer 9c exhibits strong polarization (−0.8 kcal/mol) and virtually no dispersion (−0.004 kcal/mol), trimer 9b exhibits strongly repulsive polarization and weak dispersion (+0.4 and +0.02 kcal/mol, respectively), while the dispersion (+0.09 kcal/mol) dominates over polarization (−0.03 kcal/mol) in trimer 9a. In this manner, the test set helps ensure that methods which successfully reproduce the CCSD(T) benchmark energies accurately describe the physics involved.

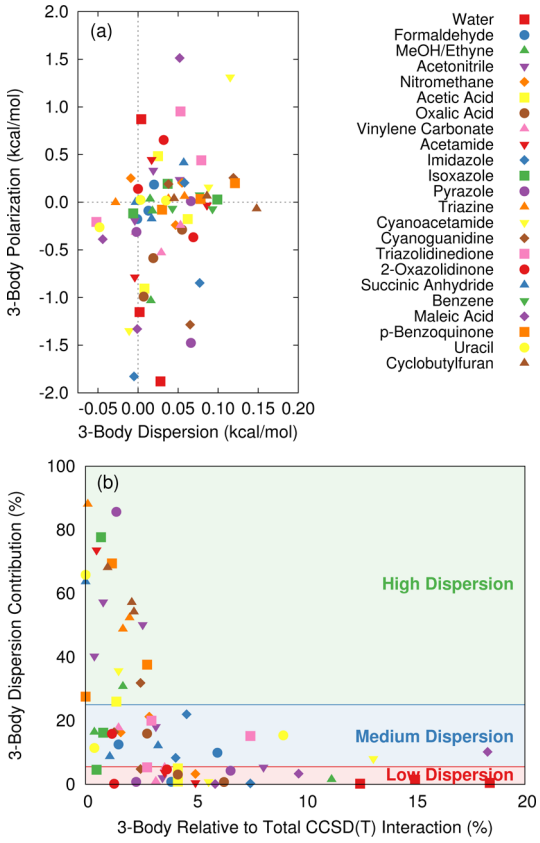

Figure 2. (a) Approximate force field decomposition of the three-body interactions into dispersion and polarization contributions. (b) Estimated percent dispersion in the three-body contribution versus the percentage of the total CCSD(T) interaction arising from three-body intermolecular interactions, ΔE^3_{rel}.

Figure 2b plots the fraction of the three-body interaction energy arising from dispersion (as computed from the AIFF energies) against ΔE^3_{rel}, the proportion of the total CCSD(T) interaction energy arising from the three-body terms (eq 3). The percent of the three-body dispersion is calculated according to

$$\%\ \text{dispersion} = \frac{|E_{disp}|}{|E_{disp}| + |E_{pol}|} \times 100 \quad (4)$$

DOI: 10.1021/acs.jctc.5b00281
J. Chem. Theory Comput. XXXX, XXX, XXX−XXX

Table 2. Errors of Tested Wavefunction Methods in the Whole Set and in the Groups of Low/Medium/High Contribution of London Dispersion:[a]

error	group	none	HF	MP2	MP3	MP2.5	CCSD	SCS-CCSD	SCS-MI-CCSD
RMSE	all	0.687	0.099	0.059	0.035	0.019	0.019	0.015	0.007
	L	1.020	0.072	0.039	0.026	0.015	0.015	0.018	0.010
	M	0.418	0.090	0.062	0.031	0.022	0.017	0.013	0.004
	H	0.192	0.132	0.076	0.048	0.020	0.024	0.009	0.004
MSE	all	0.108	−0.062	−0.039	0.022	−0.009	−0.010	−0.001	0.001
	L	0.408	−0.025	−0.015	0.012	−0.001	−0.001	0.005	0.004
	M	−0.067	−0.064	−0.045	0.018	−0.013	−0.013	−0.005	−0.002
	H	−0.102	−0.108	−0.064	0.038	−0.013	−0.020	−0.005	−0.001
MUE	all	0.460	0.077	0.045	0.026	0.014	0.014	0.010	0.005
	L	0.847	0.060	0.027	0.021	0.012	0.011	0.015	0.007
	M	0.288	0.069	0.048	0.022	0.016	0.013	0.009	0.003
	H	0.134	0.108	0.066	0.038	0.015	0.020	0.006	0.003
MUE %	all	100.0%	16.8%	9.8%	5.7%	3.1%	3.1%	2.3%	1.0%
	L	100.0%	7.0%	3.1%	2.5%	1.4%	1.3%	1.8%	0.9%
	M	100.0%	23.9%	16.6%	7.5%	5.7%	4.5%	3.1%	1.1%
	H	100.0%	80.4%	49.3%	28.4%	11.4%	14.9%	4.4%	2.2%

[a]Root mean square error (RMSE), mean signed error (MSE), and mean unsigned error (MUE) in kcal/mol and relative MUE in percent. The column "none" list the errors obtained by neglecting the three-body effects.

This form avoids anomalously large percentages in cases where the dispersion and polarization contributions have opposite signs and approximately cancel one another.

Unsurprisingly, given the relative magnitudes of the polarization and dispersion seen in Figure 2a, the importance of dispersion in the three-body terms is roughly inversely related to the overall importance of the three-body interactions ΔE^3_{rel} (Figure 2b). The largest three-body dispersion interactions (percentage-wise) occur in systems in which the net three-body interaction amounts to ∼5% or less of the total intermolecular interaction.

To facilitate the analysis described below, we partition the trimers according to the fraction of dispersion in the three-body energy. The 27 geometries in which the ATM dispersion amounts to ∼5% or less are considered "Low Dispersion", while the 21 geometries in which the dispersion ranges from ∼5−25% are considered "Medium Dispersion". The remaining 21 geometries where the three-body dispersion amounts to more than 25% of the three-body energy are classified as "High Dispersion".

Figure 2b also emphasizes the diversity within the geometries for a given trimer. In selected cases, all three geometries for a particular trimer lie in a single category. For example, the three benzene trimers all fall into the high dispersion classification, while all three water geometries exhibit low dispersion. However, in many cases, the different geometries lie in different categories. Cyanoacetamide and isoxazole, for example, each have one geometry in each category. For this reason, we classify the structures individually rather than according to their chemical composition.

3.3. Performance of Other Wave Function Methods.

Next, we examine the ability of other, less computationally demanding wave function-based electronic structure methods to reproduce the CCSD(T) three-body energies. The performance of these various methods for both the entire set and separately for each of the low, medium, and high dispersion groups is summarized in Table 2 and Figure 4. Detailed three-body energies for each structure and method are provided in Table S2 of the Supporting Information.

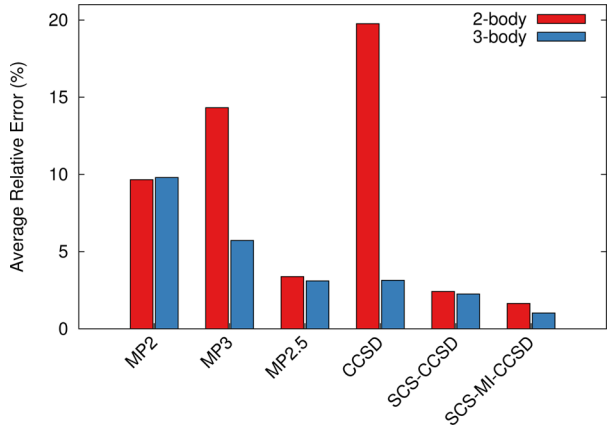

Figure 3. Comparison of relative errors of two-body interaction energies (in the S66 data set) and three-body interaction energies (this work).

To begin, Figure 3 compares the relative errors in the three-body energies here to those obtained using the same methods for the two-body energies in the S66 data set of interaction energies.[54,55] As system sizes grow, the number of three-body interactions and the magnitude of their overall contribution to the total energies increases. Understanding how the relative errors for three-body energies compare to those for two-body interactions provides insight into how various methods will perform for larger systems. As shown in Figure 3, the average relative three-body errors are comparable to or smaller than the two-body ones, which suggests that the errors should behave well as three body interactions become more important.

Focusing on the three-body contributions now, we note that neglecting the three-body interaction energies entirely leads to a root-mean-square error (RMSE) of 0.687 kcal/mol. A significant fraction of the three-body contribution arises from polarization. Accordingly, applying even the simple HF model reduces the RMSE to 0.099 kcal/mol. Of course, HF does not account for dispersion, and the errors in the three-body energies increase as the relative size of the dispersion energy grows. The missing three-body dispersion corrections are

DOI: 10.1021/acs.jctc.5b00281
J. Chem. Theory Comput. XXXX, XXX, XXX−XXX

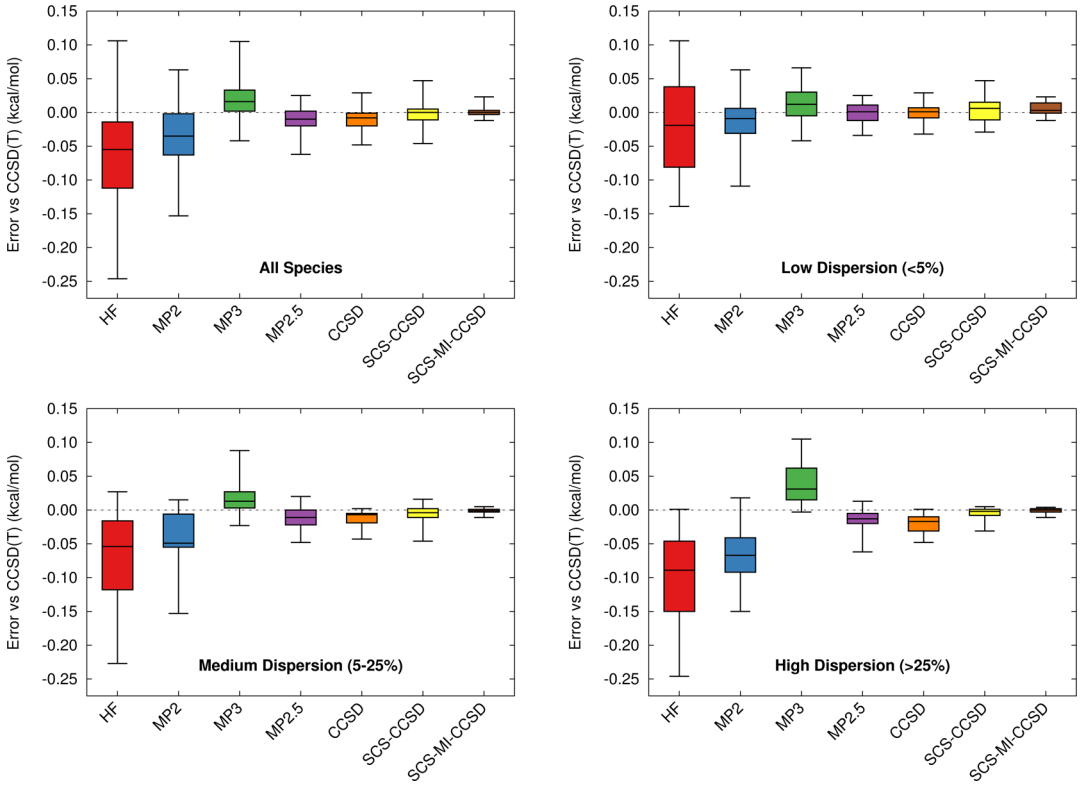

Figure 4. Distribution of errors in the three-body energies for various wave function models relative to the CCSD(T) benchmarks, in kcal/mol. The box plots show the errors over all species in the test set and partitioned according the low/medium/high dispersion relative amount of dispersion categories defined in Table 1. For each box, the central line represents the median error, the box includes 50% of the errors, and the whiskers show the largest errors.

frequently repulsive, so HF often overestimates the three-body energy, as indicated by the negative values of the mean signed error (MSE) in Table 2 and in the box plots shown in Figure 4.

MP2 improves upon the HF treatment of polarization somewhat, reducing the RMSE to 0.059 kcal/mol, but it still systematically overbinds the trimers. Like for HF, the MP2 overbinding becomes increasingly pronounced as the relative size of the dispersion energy grows (Figure 4). The MSE quadruples from −0.015 kcal/mol in the low-dispersion subset to −0.064 kcal/mol in the high-dispersion subset. This systematic overbinding in high-dispersion cases is similar to the overbinding observed for MP2 in two-body (dimer) interactions,[54] though the reasons for the overbinding are very different. For pairwise interactions, the poor quality of the uncoupled HF dispersion in MP2 leads to overbinding.[75] For three-body interactions, on the other hand, MP2 overbinds because it does not include the (frequently repulsive) three-body dispersion.[30] Note that spin-component scaling[76−78] cannot physically compensate for the missing three-body dispersion energies, either.

Intermolecular three-body dispersion first appears in MP3. Accordingly, the RMSE for MP3 drops significantly to 0.035 kcal/mol. Analogously to two-body interaction energies, MP3 systematically underbinds. However, the relative error in the three-body energies is smaller than the one in pairwise interactions. The dependence on the amount of dispersion is less pronounced than in MP2, but it has an opposite sign. MP3 overestimates the destabilizing contribution of three-body dispersion (it would be partially canceled by the fourth-order dispersion contribution, for instance[60,79,80]), as a result, the mean signed error is positive in all three groups.

The scaled variant of MP3, MP2.5, exploits the cancellation of errors between MP2 and MP3 and thus offers much better results. The RMSE is 0.019 kcal/mol, the relative error is only 3.1%. Of the methods tested, MP2.5 is the least expensive option that provides significant improvement over MP2. The results confirm our very good experience with this method in calculations of interaction energies in various systems.[34] This is the first method which can be recommended for quantitative analysis of three-body energies when more expensive calculations are not tractable.

The performance of CCSD is somewhat surprising. CCSD yields rather poor two-body interaction energies which are often worse than MP2 (see Figure 3). In contrast, the CCSD describes three-body energies very well, with RMSE of 0.019 kcal/mol. On the other hand, CCSD provides little or no improvement relative to MP2.5, despite its significantly higher computational cost (both methods scale as $O(N^6)$, but CCSD is iterative).

The CCSD results can be improved further by introducing empirical scaling of the spin components of the correlation energy. Using the original SCS-CCSD parameters, which were developed for describing reaction energies, the RMSE drops only slightly to 0.015 kcal/mol. The spin-component-scaled CCSD model parametrized specifically for noncovalent interactions, SCS-MI-CCSD, leads to much more significant improvements: the RMSE is 0.007 kcal/mol and the relative error is only 1.0%. Analogously to the situation in two-body interaction energies, this method yields results that are practically equivalent to full CCSD(T) calculations, while avoiding the expensive evaluation of the triples. Additionally, the spin-component-scaled CCSD models are the only two

DOI: 10.1021/acs.jctc.5b00281
J. Chem. Theory Comput. XXXX, XXX, XXX−XXX

methods for which the relative error is practically independent of the nature of the interactions. In all other cases, the relative error in the group with the highest contribution of dispersion is an order of magnitude higher than in the group of the most polar ones.

To view these results another way, Figure 5 plots the correlation between the error in each trimer structure and the

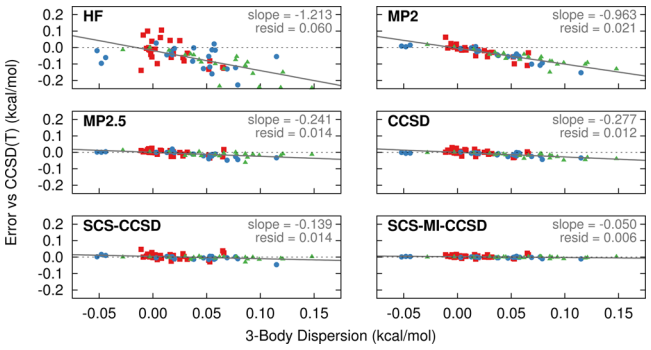

Figure 5. Correlation between the estimated AIFF three-body dispersion and the error relative to the CCSD(T) benchmarks for each trimer geometry. Low, medium, and high dispersion structures (defined in Table 1) are indicated as red squares, blue circles, and green triangles, respectively. The least-squares fit line, its slope, and the rms of the residuals are shown in gray.

size of the three-body AIFF dispersion contribution. If (1) a model described all three-body interactions except three-body dispersion perfectly and (2) the force field model gave a perfect description of the three-body dispersion, then models like HF and MP2, which do not include three-body dispersion, would lie exactly along a line with slope of −1 in these graphs. On the other hand, if both criteria were true and a model captures dispersion perfectly, it would have a slope of zero.

Obviously neither of these criteria is precisely met. We do observe, however, that the slope of the best fit line for SCS-MI-CCSD is very nearly zero (−0.05), and the data points exhibit very little scatter around this line. The results further demonstrate the uniformly excellent performance of SCS-MI-CCSD across a wide variety of three-body interaction types and sizes.

In contrast, the HF errors are only moderately correlated with the three-body dispersion. In fact, HF shows relatively large scatter even for the low dispersion cases, indicating that HF both fails to describe dispersion and exhibits nontrivial polarization errors. On the other hand, the MP2 data falls reasonably well along a line with slope of −0.96, close to the idealized slope of −1, and with much less scatter than the HF errors. In other words, MP2 improves substantially upon the HF treatment of polarization, but it lacks three-body dispersion. Accordingly, the MP2 errors grow nearly linearly with increasing magnitude of the three-body dispersion.

MP2.5, CCSD, and SCS-CCSD all reduce the scatter about the best fit line further, and the slopes slowly approach the near-zero slope of SCS-MI-CCSD. Those models include three-body dispersion (unlike HF and MP2) and further refine the treatment of polarization, leading to improved agreement with CCSD(T).

Overall, of the wave function methods considered here, MP2.5 offers the best compromise between accuracy and computational efficiency with its noniterative $O(N^6)$ scaling. If higher accuracy is needed, SCS-MI-CCSD provides near-CCSD(T) quality with iterative $O(N^6)$ cost. Both are substantially less computationally demanding than the $O(N^7)$ effort required to evaluate the perturbative triples contribution.

3.4. Performance of DFT Methods. To examine the performance of DFT methods for three-body interactions, we have chosen a set of commonly used DFT functionals that represent different families: 1) pure generalized gradient approximation (GGA) functionals B-LYP and PBE, 2) hybrid functionals B3-LYP, Becke half and half LYP (BH-LYP), and PBE0, 3) range-separated hybrid CAM-B3-LYP, 4) meta-GGA functional TPSS, 5) meta-hybrids M06-2X and M06-HF, and 6) double hybrid B2-PLYP. For comparison, we list also the HF-D3 results.

The authors of the DFT-D3 method recommend using the def2-QZVP basis set.[81] Although this basis set is rather large, we found that the absence of diffuse basis functions means that the three-body energies calculated in this basis set are not

Table 3. Errors of Tested DFT (and HF) Methods with the Three-Body D3 Dispersion Correction, Calculated in the Whole Set and in the Groups of Low/Medium/High Contribution of London Dispersion[a]

error	group	B-LYP	B3-LYP	BH-LYP	CAM-B3-LYP	PBE	PBE0	TPSS	M06-2X	M06-HF	B2-PLYP	HF
RMSE	all	0.111	0.069	0.045	0.046	0.147	0.080	0.109	0.192	0.248	0.050	0.076
	L	0.131	0.083	0.044	0.052	0.126	0.075	0.111	0.114	0.210	0.042	0.065
	M	0.081	0.054	0.051	0.051	0.156	0.087	0.110	0.206	0.249	0.047	0.076
	H	0.107	0.061	0.038	0.026	0.164	0.079	0.104	0.249	0.289	0.061	0.089
MSE	all	−0.084	−0.046	−0.018	−0.008	0.093	0.043	0.057	−0.112	−0.169	−0.028	−0.038
	L	−0.088	−0.052	−0.018	−0.013	0.033	0.012	0.005	−0.014	−0.076	−0.026	−0.015
	M	−0.070	−0.035	−0.012	−0.003	0.117	0.058	0.086	−0.160	−0.208	−0.027	−0.042
	H	−0.091	−0.050	−0.024	−0.006	0.144	0.068	0.094	−0.189	−0.250	−0.030	−0.065
MUE	all	0.086	0.052	0.033	0.034	0.122	0.068	0.093	0.137	0.187	0.038	0.059
	L	0.094	0.061	0.031	0.043	0.092	0.059	0.084	0.071	0.118	0.035	0.053
	M	0.070	0.042	0.040	0.037	0.134	0.076	0.099	0.161	0.212	0.035	0.061
	H	0.092	0.052	0.030	0.020	0.149	0.072	0.098	0.199	0.250	0.045	0.065
MUE %	all	18.7%	11.4%	7.3%	7.5%	26.6%	14.8%	20.2%	29.8%	40.6%	8.2%	12.8%
	L	11.1%	7.2%	3.7%	5.1%	10.9%	6.9%	10.0%	8.4%	13.9%	4.1%	6.2%
	M	24.3%	14.5%	13.7%	12.9%	46.6%	26.4%	34.2%	55.8%	73.6%	12.0%	21.3%
	H	68.8%	38.4%	22.5%	14.8%	111.2%	53.9%	72.9%	148.5%	186.4%	33.5%	48.4%

[a]Root mean square error (RMSE), mean signed error (MSE), and mean unsigned error (MUE) in kcal/mol and relative MUE in percent.

DOI: 10.1021/acs.jctc.5b00281
J. Chem. Theory Comput. XXXX, XXX, XXX−XXX

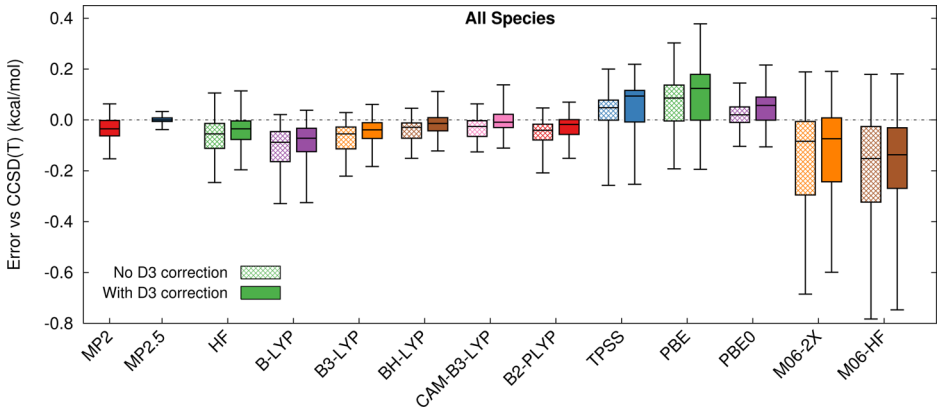

Figure 6. Distribution of errors in the three-body energies for HF and various DFT functionals relative to the CCSD(T) benchmarks, in kcal/mol. For HF and DFT, the hashed boxes correspond to no dispersion correction, while the solid boxes include the D3 correction. MP2 and MP2.5 errors are included to facilitate comparison with Figure 4.

converged to the desired accuracy. Rather than switching to the def2-QZVPD basis, we use the aug-cc-pVQZ (abbreviated here as aQZ) basis set because it is the one used also for the HF calculations that form the basis for the benchmark calculations; this allows for one-to-one comparison of the DFT calculations both to the CCSD(T) benchmark and to the other wave function methods. The basis set convergence of the DFT methods was assessed further by analyzing the series of aDZ, aTZ, and aQZ basis sets. In the aQZ basis, the BSSE is very small; in B-LYP/aQZ calculations, the root-mean-square difference between three-body energies calculated with and without counterpoise correction is only 0.007 kcal/mol. This justifies the neglect of the counterpoise correction in all the DFT calculations presented here.

The results of the DFT-D3 calculations are available in Table S3 in the Supporting Information. Multiple statistical error measures summarize that data in Table 3, and the error distributions are presented as box plots in Figure 6. Looking at Figure 6, two features are immediately obvious. First, the DFT errors are generally large compared to those obtained with the wave function methods like MP2 or MP2.5. In fact, only four of the tested dispersion-corrected density functionals perform better than HF-D3: The best results were obtained with BH-LYP (RMSE 0.045 kcal/mol), followed by CAM-B3-LYP (RMSE 0.046 kcal/mol), B2-PLYP (RMSE 0.050 kcal/mol), and B3-LYP (RMSE 0.069 kcal/mol). These errors are comparable to those obtained with MP2 (0.059 kcal/mol), in marked contrast from the two-body case where DFT-D3 models outperform MP2 significantly.[82] In relative terms, the DFT-D3 three-body errors range from 7 to 11%. The negative mean signed error indicates that all four of these functionals overestimate the stabilizing three-body contributions which largely arise from the description of polarization. The remaining functionals, B-LYP, PBE, PBE0, TPSS, M06-2X, and M06-HF, yield larger errors. Out of these, PBE, PBE0, and TPSS have positive mean signed error, which will be discussed later. Note that the relative 3-body errors here are substantially larger than those observed for 2-body interactions for many of the functionals (Figure 7), in marked contrast from the wave function case (Figure 3). This result is potentially troubling for the performance of these functionals to larger systems where the errors in the many-body contributions out-weigh pairwise interactions.

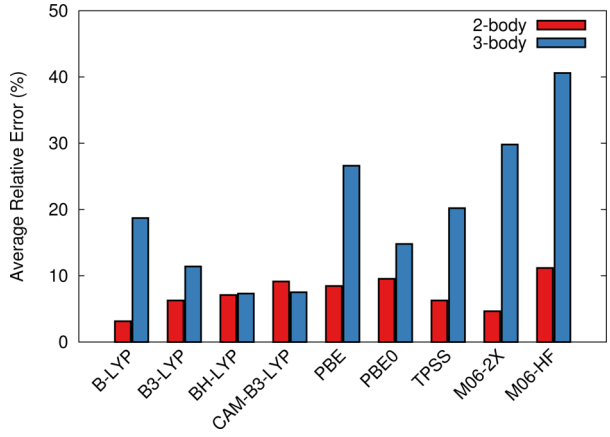

Figure 7. Comparison of relative errors of two-body interaction energies (in the S22 data set) and three-body interaction energies (this work) for various density functionals corrected with the D3 dispersion correction.

Second, the D3 dispersion correction often (but not always) improves the results, but its impact is relatively small in small molecules like these. It helps the functionals that predict 3-body interactions which are too attractive, but it increases the errors for functionals like PBE, PBE0, and TPSS, which are too repulsive. Previous workers have made similar observations about ATM-type three-body dispersion corrections to DFT.[10−12,14,65] Compared to the wave function methods shown in Figure 5, the DFT-D3 errors correlate poorly with the amount of AIFF 3-body dispersion (see Figures S2−S4 in the Supporting Information). In other words, missing three-body dispersion is not the dominant source of error in the DFT calculations. Rather, the most important trend can be observed when moving from GGA to hybrid functionals—from B-LYP to B3-LYP (contains 20% of HF exchange) and BH-LYP (50% HF exchange) or from PBE to PBE0 (25% HF exchange). In these series, the errors systematically decrease as the fraction of exact exchange increases. The range-separated CAM-B3-LYP contains up to 65% of HF exchange, and it also yields very good results that are similar to those from BH-LYP.

Plots of the errors versus the AIFF-estimated three-body polarization in Figure 8 demonstrate how increasing the amount of exact exchange in this family of functionals improves the treatment of polarization. Increasing HF exchange generally reduces the dependence of the error on the magnitude of the

DOI: 10.1021/acs.jctc.5b00281
J. Chem. Theory Comput. XXXX, XXX, XXX−XXX

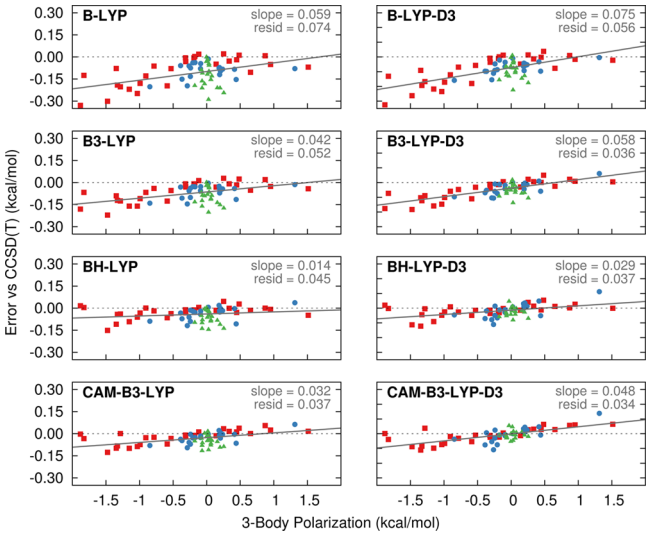

Figure 8. Correlation between the estimated AIFF three-body polarization and the three-body error for each trimer geometry. Low, medium, and high dispersion structures (defined in Figure 2b) are indicated as red squares, blue circles, and green triangles, respectively.

polarization contribution (i.e., slopes closer to zero) and reduces the scatter about the best fit lines. The good results of the double-hybrid B2-PLYP functional can also be explained by the large fraction of HF exchange it uses (53%) rather than the use of MP2-like correlation. The only exception is M06-2X, which exhibits very large error (RMSE 0.192 kcal/mol). Increasing the exact exchange to 100% in M06-HF makes the error even worse (0.248 kcal/mol).

We attribute these DFT results to two major sources of error. The first is the delocalization error (also referred to as many-body self-interaction error) in the underlying density functionals. Approximate semilocal density functionals frequently predict an electron density that is too delocalized,[83,84] and this leads to an overestimation of the molecular polarizability. Systems with strong intermolecular interactions tend to exhibit more delocalized electron densities, and the artificial delocalization becomes increasingly exacerbated in systems with delocalized densities. However, this delocalization error is not limited to systems with strong polarization effects. The local density approximation (LDA) functional significantly overestimates the delocalization of the electron density in the argon trimer as well,[85] for instance.

GGA functionals exhibit substantial delocalization error, and mixing a fraction of exact exchange into the density functional tends to decrease the delocalization error. This explains the reduction in errors from B-LYP to B3-LYP (20% exact exchange) to BH-LYP (50% exact exchange) or from PBE to PBE0 (25% exact exchange), for example. Hartree−Fock theory, on the other hand, predicts excessively localized electron densities. Previous work suggests that BH-LYP, with 50% exact exchange, provides an effective balance between these extremes,[86] as reflected in the low errors observed here for that functional.

Following the discussion of ref 86, we compute the intermolecular delocalization index for each trimer, which is defined as the sum of the Bader delocalization indices[87−89] for each possible pairs of atoms located on two separate molecules. The delocalization indices were computed at the BH-LYP/aug-cc-pVTZ level using the AIMAll program.[90] BH-LYP provides a relatively balanced degree of delocalization,[86] and the

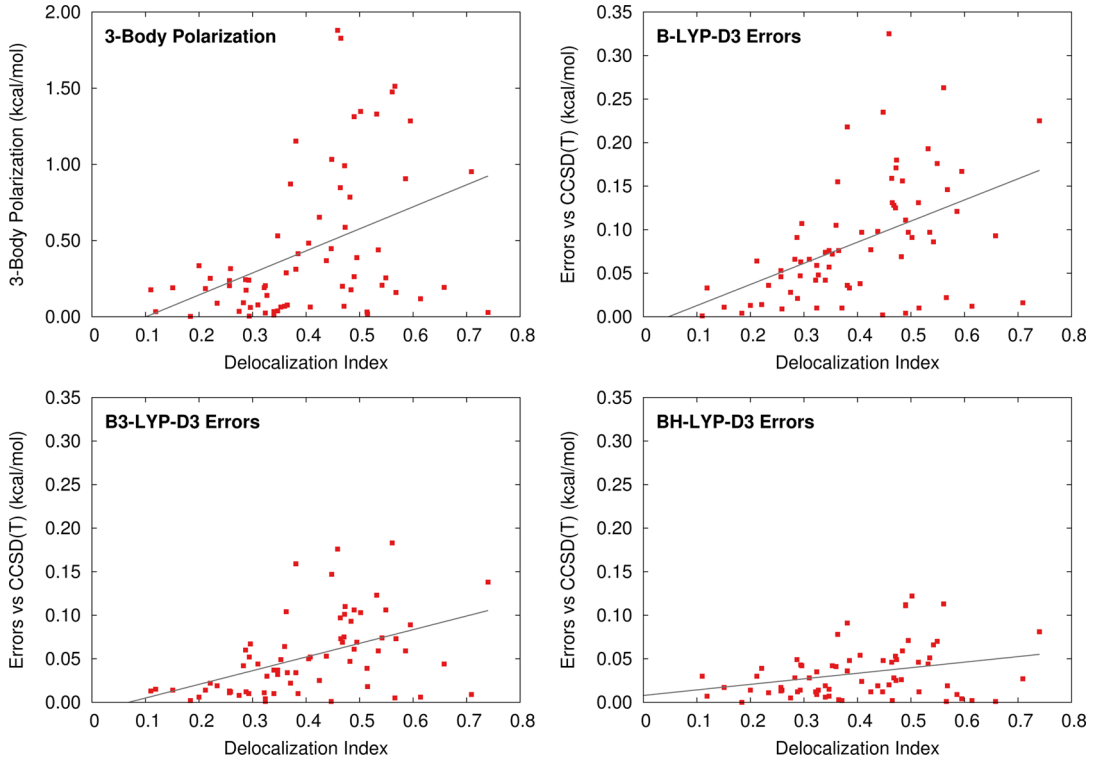

Figure 9. Correlation between BH-LYP intermolecular delocalization indices and the force field polarization and with the errors B-LYP-D3, B3-LYP-D3, and BH-LYP-D3 errors. The linear regression lines are plotted as a visual guide.

DOI: 10.1021/acs.jctc.5b00281
J. Chem. Theory Comput. XXXX, XXX, XXX−XXX

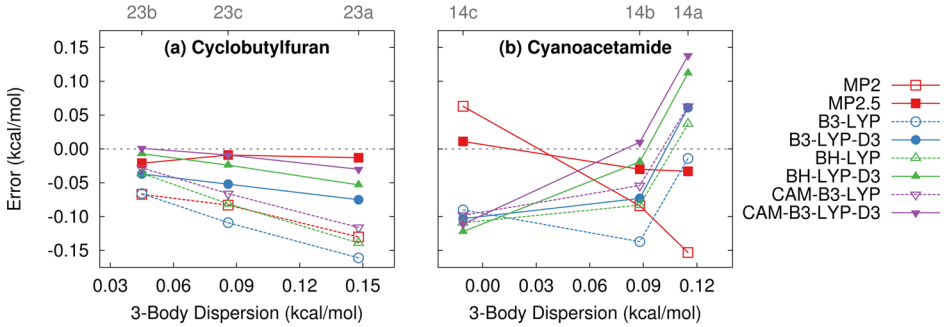

Figure 10. Errors in the three-body energies relative to CCSD(T) for (a) cyclobutylfuran and (b) cyanoacetamide versus the estimated three-body dispersion, in kcal/mol. The numbers above the graphs indicate the structure numbers (see the Supporting Information).

delocalization indices are well converged with respect to basis set size already in the aug-cc-pVTZ basis.

While the correlation between the strength of the three-body interaction and the intermolecular delocalization index is less strong than it was for the binding energies in halogen-bonded dimers with a high degree of charge transfer,[86] Figure 9 shows that the trimers with strong three-body polarization generally exhibit higher delocalization. It also demonstrates that the errors in these species are somewhat correlated with the magnitude of the delocalization—larger intermolecular delocalization indices often correspond with larger errors. The delocalization error decreases in the series B-LYP, B3-LYP, and BH-LYP (see Figure S6 in the Supporting Information). The errors in the three-body energies also decrease accordingly. In other words, a sizable portion of the error observed for the density functionals stems from delocalization error.

Note that HF three-body interactions also exhibit negative MSE, similar to the hybrid functionals. The problem for HF stems from the lack of electron−electron correlation, which leads to an inaccurate description of the polarization, rather than just the missing dispersion. This is demonstrated by the poor correlation of the HF results with the AIFF dispersion (see Figure 5 and also Figures S4 and S5 in the Supporting Information).

The second major source of error in the DFT calculations appears to be the exchange functional. Delocalization error alone does not explain the opposite signs of the mean errors for PBE versus B-LYP, for instance. Both functionals exhibit similar delocalization error (see Figure S6 in the Supporting Information) and overestimate polarizabilities by a similar amount.[84] So one might expect similar overestimation of the polarization component of the three-body energies for both functionals.

In reality, these two functionals differ in their descriptions of intermolecular interactions. For two-body interactions, PBE is too attractive, while B-LYP is overly repulsive, as has been demonstrated for rare gas dimers[91] and other systems. This behavior in dimers has been ascribed to the different treatment of exchange repulsion in the various functionals.[91]

For the three-body energies, we observe the opposite trend in the errors: in the absence of a dispersion correction, B-LYP overbinds, while PBE underbinds. Gillan recently examined the behavior of several GGA functionals for treating the three-body interactions in rare gas and water trimers.[92] He also observed opposite signs of the two- and three-body errors, which he attributes to the partial back-transfer of electrons from higher to lower densities in the three-body contribution. He rationalizes these behaviors based on the form of the GGA exchange functionals.

Given opposite signs of the two-body and three-body errors in these two functionals, one can expect some error compensation in larger systems. However, it is unclear how systematic this error cancellation is, so it should not be relied on. Instead, better results could be obtained with other, more accurate functionals that exhibit negative mean-signed errors which can be corrected through the incorporation of a three-body dispersion correction.

To obtain additional insights into the performance of the DFT functionals, consider the cyclobutylfuran and cyanoacetamide trimer errors in Figure 10. In cyclobutylfuran, the three-body dispersion increases steadily as the packing density of the molecules increases (geometries 23b → 23c → 23a), while the polarization ranges from attractive (23a) to moderately repulsive (23b) to even more repulsive (23c). The MP2 error correlates reasonably well with the amount of the three-body dispersion, and moving to MP2.5 largely eliminates the errors across all three geometries. B3-LYP, BH-LYP, and CAM-B3-LYP also correlate fairly well with the missing three-body dispersion. The errors generally shrink as the amount of exact exchange in the functional increases. Adding the D3 dispersion correction improves the results for all three functionals, but the dispersion correction appears to be too weak to fully correct the results (particularly for B3-LYP).

In cyanoacetamide, the dispersion becomes more repulsive along structures 14c → 14b → 14a. At the same time, the AIFF polarization ranges from strongly attractive (−1.3 kcal/mol) toward strongly repulsive (+1.3 kcal/mol). Once again, the MP2 errors correlate somewhat with the amount of missing three-body dispersion, and MP2.5 helps correct the residual problems. In contrast, the B3-LYP, BH-LYP, and CAM-B3-LYP errors are nearly anticorrelated with the three-body dispersion. The other functionals tested perform equally poorly or worse for cyanoacetamide. Adding D3 dispersion only makes the slope of the errors more positive.

In other words, the main source of error for the DFT-D3 results appears to come from the polarization and/or exchange terms. The large size of these polarization errors makes it difficult to assess the accuracy of the dispersion correction itself. The overall results are strongly affected by the cancellation of errors between the polarization (which is on average stabilizing) and dispersion (which is typically destabilizing). Some of the functionals (PBE, PBE0, and TPSS) which have positive MSE even yield lower errors when the dispersion correction is omitted, as has been recognized previously.[85] On the other hand, as hinted by the cyclobutylfuran example, the

DOI: 10.1021/acs.jctc.5b00281
J. Chem. Theory Comput. XXXX, XXX, XXX−XXX

three-body D3 correction (at least in its original short-range damping parametrization) might be too weak for the better-performing functionals, leading to overstabilization of the three-body contribution. The difficulties in defining an appropriate three-body dispersion damping function have been noted previously.[10]

To explore this issue further, we vary the strength of the D3 dispersion correction at short-range where it is most important by adjusting the scaling of the radii (parameter s_r) in the damping function. The parameter was set to values ranging from 0.9 to 1.5 (the original value is 1.33; the lower the number, the weaker is the damping). For comparison, the D3 dispersion correction was calculated without any damping at one extreme, and the results without the D3 correction represent the other one. The results are plotted in Figure 11.

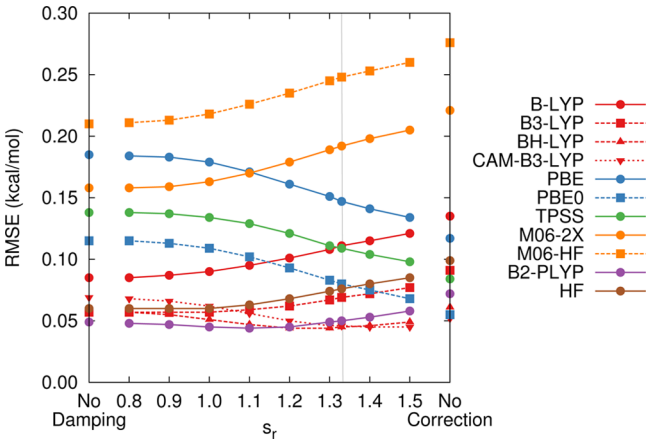

Figure 11. Error of the DFT-D3 calculations as a function of radii scaling factor in the damping function in the three-body term.

For BH-LYP and CAM-B3-LYP, the default s_r is close to the optimal value. For B2-PLYP, B-LYP, B3-LYP, and HF, the errors would be reduced if weaker damping were applied, since more repulsive dispersion would help compensate for the overestimated polarization. M06-2X and M06-HF would also benefit from less damping, though the errors would remain large. PBE, PBE0, and TPSS suffer the opposite problem, underestimation of the polarization, and the best results are achieved when the dispersion correction is not used at all. Further improvements could be probably achieved by changing other properties of the damping function. However, it is important to recognize that such modifications to the dispersion correction are often compensating for the polarization errors, and a proper fix should focus on improving the treatment of polarization first.

4. CONCLUSION

Effectively treating many-body interactions becomes more important as quantum chemistry moves toward larger molecules and condensed-phase systems. To assess the ability of quantum chemistry methods to treat such interactions, we have developed the 3B-69 benchmark test set of three-body intermolecular interactions computed with complete-basis-set CCSD(T) on three geometries for each of 23 different trimers. Obtaining high accuracy results on these benchmarks requires methods capable of describing three-body polarization and dispersion effects reliably across a variety of chemical species and geometric arrangements. The typical three-body interaction energy in the 3B-69 set accounts for about 4% of the total trimer interaction energy, though it approaches 20% in some cases. Of the three-body energies, dispersion accounts for ∼5% or less of the interaction in about a third of the cases, ∼5−25% in another third, and >25% in the remaining third.

Testing less computationally expensive wave function and density functional methods against these CCSD(T) benchmarks revealed a number of interesting features:

1. The relative sizes of the errors in the three-body energies observed for wave function-based methods are comparable to the relative errors observed when using the same methods for two-body interactions.
2. MP2 performs notably better than HF for three-body polarization, but it lacks three-body dispersion.
3. At noniterative $O(N^6)$ cost, MP2.5 is the least-expensive wave function model tested that describes both three-body polarization and dispersion contributions well.
4. SCS-MI-CCSD reproduces the three-body benchmark energies with near-quantitative accuracy.
5. The DFT functionals examined here exhibit errors in the many-body polarization and exchange that frequently outweigh errors arising from missing three-body dispersion. This error stems from delocalization errors in the underlying functionals and the form of the exchange functionals. Functionals like BH-LYP with a larger proportion of exact exchange perform best, but they still exhibit problematic behaviors.
6. Given the large errors in the underlying density functionals, disentangling the DFT errors due to the treatment of three-body dispersion is difficult. However, the D3 dispersion correction may somewhat underestimate the size of the three-body dispersion for functionals like B3-LYP. On the other hand, functionals like PBE, PBE0, and TPSS predict three-body contributions that are generally too repulsive, and adding three-body dispersion only makes the overall errors worse.

Overall, the benchmark data provided here suggests that while the reliable treatment of three-body interactions is feasible with existing methodology, there remains considerable room for the development of improved low-cost models capable of describing these effects reliably. For density functional theory in particular, addressing the issues of many-body exchange, delocalization error, and the treatment of many-body polarization should probably be given higher priority than including three-body dispersion corrections.

■ ASSOCIATED CONTENT

Supporting Information

Cartesian coordinates, molecular images, results and error correlation plots for all the methods tested on all 69 trimers, and a plot comparing delocalization indices across several density functionals are provided. The Supporting Information is available free of charge on the ACS Publications website at DOI: 10.1021/acs.jctc.5b00281.

■ AUTHOR INFORMATION

Corresponding Author

*E-mail: gregory.beran@ucr.edu.

Notes

The authors declare no competing financial interest.

DOI: 10.1021/acs.jctc.5b00281
J. Chem. Theory Comput. XXXX, XXX, XXX−XXX

■ ACKNOWLEDGMENTS

The work is part of research project RVO:61388963 of the IOCB AS CR. Funding for this work from the National Science Foundation CHE-1362465 (Y.H. and G.B.), Czech Science Foundation P208/13/01214P (J.Ř.) and P208/12/G016 (J.Ř. and P.H.), and supercomputer time from XSEDE TG-CHE110064 (Y.H. and G.B.) are gratefully acknowledged.

■ REFERENCES

(1) Beran, G. J. O.; Nanda, K. *J. Phys. Chem. Lett.* **2010**, *1*, 3480−3487.
(2) Kamiya, M.; Hirata, S.; Valiev, M. *J. Chem. Phys.* **2008**, *128*, 074103.
(3) Wen, S.; Beran, G. J. O. *J. Chem. Theory Comput.* **2011**, *7*, 3733−3742.
(4) Wen, S.; Beran, G. J. O. *J. Chem. Theory Comput.* **2012**, *8*, 2698−2705.
(5) Podeszwa, R.; Rice, B. M.; Szalewicz, K. *Phys. Rev. Lett.* **2008**, *101*, 115503.
(6) DiStasio, R. A.; von Lilienfeld, O. A.; Tkatchenko, A. *Proc. Nat. Acad. Sci.* **2012**, *109*, 14791−14795.
(7) Reilly, A. M.; Tkatchenko, A. *J. Phys. Chem. Lett.* **2013**, *4*, 1028−1033.
(8) Reilly, A. M.; Tkatchenko, A. *J. Chem. Phys.* **2013**, *139*, 024705.
(9) Marom, N.; DiStasio, R. A.; Atalla, V.; Levchenko, S.; Reilly, A. M.; Chelikowsky, J. R.; Leiserowitz, L.; Tkatchenko, A. *Angew. Chem., Int. Ed.* **2013**, *52*, 6629−32.
(10) Otero-de-la Roza, A.; Johnson, E. R. *J. Chem. Phys.* **2013**, *138*, 054103.
(11) Grimme, S.; Antony, J.; Ehrlich, S.; Krieg, H. *J. Chem. Phys.* **2010**, *132*, 154104.
(12) Grimme, S. *J. Chem. Eur.* **2012**, *18*, 9955−9964.
(13) Risthaus, T.; Grimme, S. *J. Chem. Theory Comput.* **2013**, *9*, 1580−1591.
(14) Moellmann, J.; Grimme, S. *J. Phys. Chem. C* **2014**, *118*, 7615−7621.
(15) Brandenburg, J. G.; Grimme, S. *Top. Curr. Chem.* **2014**, *345*, 1−23.
(16) Kennedy, M. R.; McDonald, A. R.; DePrince, A. E.; Marshall, M. S.; Podeszwa, R.; Sherrill, C. D. *J. Chem. Phys.* **2014**, *140*, 121104.
(17) Yang, J.; Hu, W.; Usvyat, D.; Matthews, D.; Schutz, M.; Chan, G. K.-L. *Science* **2014**, *345*, 640−643.
(18) Jurečka, P.; Šponer, J.; Černý, J.; Hobza, P. *Phys. Chem. Chem. Phys.* **2006**, *8*, 1985−1993.
(19) Gráfová, L.; Pitoňák, M.; Řezáč, J.; Hobza, P. *J. Chem. Theory Comput.* **2010**, *6*, 2365−2376.
(20) Řezáč, J.; Riley, K. E.; Hobza, P. *J. Chem. Theory Comput.* **2011**, *7*, 2427−2438.
(21) Řezáč, J.; Riley, K. E.; Hobza, P. *J. Chem. Theory Comput.* **2011**, *7*, 3466−3470.
(22) Řezáč, J.; Riley, K. E.; Hobza, P. *J. Chem. Theory Comput.* **2012**, *8*, 4285−4292.
(23) Faver, J. C.; Benson, M. L.; He, X.; Roberts, B. P.; Wang, B.; Marshall, M. S.; Kennedy, M. R.; Sherrill, C. D.; Merz, K. M. *J. Chem. Theory Comput.* **2011**, *7*, 790−797.
(24) Otero-de-la Roza, A.; Johnson, E. R. *J. Chem. Phys.* **2012**, *137*, 054103.
(25) Sedlak, R.; Janowski, T.; Pitoňák, M.; Řezáč, J.; Pulay, P.; Hobza, P. *J. Chem. Theory Comput.* **2013**, *9*, 3364−3374.
(26) Ambrosetti, A.; Alfe, D.; Distasio, R. A.; Tkatchenko, A. *J. Phys. Chem. Lett.* **2014**, *5*, 849−855.
(27) Fang, T.; Li, W.; Gu, F.; Li, S. *J. Chem. Theory Comput.* **2015**, *11*, 91−98.
(28) Axilrod, P. M.; Teller, E. *J. Chem. Phys.* **1943**, *11*, 299−300.
(29) Muto, Y. *Proc. Phys.-Math. Soc. Jpn.* **1943**, *17*, 629−631.
(30) Chalasinski, G.; Szczesniak, M. M.; Kendall, R. A. *J. Chem. Phys.* **1994**, *101*, 8860−8869.
(31) Takatani, T.; Hohenstein, E. G.; Sherrill, C. D. *J. Chem. Phys.* **2008**, *128*, 124111.
(32) Pitoňák, M.; Řezáč, J.; Hobza, P. *Phys. Chem. Chem. Phys.* **2010**, *12*, 9611.
(33) Pitoňák, M.; Neogrády, P.; Černý, J.; Grimme, S.; Hobza, P. *ChemPhysChem* **2009**, *10*, 282−289.
(34) Sedlák, R.; Riley, K. E.; Řezáč, J.; Pitoňák, M.; Hobza, P. *ChemPhysChem* **2013**, DOI: 10.1002/cphc.201200850.
(35) Morrison, I.; Li, J.-C.; Jenkins, S.; Xantheas, S. S.; Payne, M. C. *J. Phys. Chem. B* **1997**, *101*, 6146−6150.
(36) Becke, A. D. *J. Chem. Phys.* **1993**, *98*, 5648−5652.
(37) Civalleri, B.; Zicovich-Wilson, C. M.; Valenzano, L.; Ugliengo, P. *CrystEngComm* **2008**, *10*, 405−410.
(38) Schafer, A.; Horn, H.; Ahlrichs, R. *J. Chem. Phys.* **1992**, *97*, 2571.
(39) Dovesi, R.; Saunders, V. R.; Roetti, C.; Orlando, R.; Zicovich-Wilson, C. M.; Pascale, F.; Civalleri, B.; Doll, K.; Harrison, N. M.; Bush, I. J.; D'Arco, P.; Llunell, M.; Science, C.; Technologies, A. *CRYSTAL09 User's Manual*; University of Torino: Torino, 2009.
(40) Chisholm, J. A.; Motherwell, W. D. S. *J. Appl. Crystallogr.* **2005**, *38*, 228−231.
(41) Valiron, P.; Mayer, I. *Chem. Phys. Lett.* **1997**, *275*, 46−55.
(42) Alvarez-Idaboy, J. R.; Galano, A. *Theor. Chem. Acc.* **2010**, *126*, 75−85.
(43) Mentel, L. M.; Baerends, E. J. *J. Chem. Theory Comput.* **2014**, *10*, 252−267.
(44) van Duijneveldt, F. B.; van Duijneveldt-van de Rijdt, J. G. C. M.; van Lenthe, J. H. *Chem. Rev.* **1994**, *94*, 1873−1885.
(45) Burns, L. A.; Marshall, M. S.; Sherrill, C. D. *J. Chem. Theory Comput.* **2014**, *10*, 49−57.
(46) Richard, R. M.; Lao, K. U.; Herbert, J. M. *Acc. Chem. Res.* **2014**, *47*, 2828−36.
(47) Ouyang, J. F.; Cvitkovic, M. W.; Bettens, R. P. A. *J. Chem. Theory Comput.* **2014**, *10*, 3699−3707.
(48) Řezáč, J. Cuby 4, software framework for computational chemistry. http://cuby4.molecular.cz/ (accessed May 21, 2015).
(49) Tsuzuki, S.; Honda, K.; Uchimaru, T.; Mikami, M.; Tanabe, K. *J. Am. Chem. Soc.* **2002**, *124*, 104−112.
(50) Jurečka, P.; Hobza, P. *Chem. Phys. Lett.* **2002**, *365*, 89−94.
(51) Dunning, T. H. *J. Chem. Phys.* **1989**, *90*, 1007.
(52) Woon, D. E.; Dunning, T. H. *J. Chem. Phys.* **1994**, *100*, 2975.
(53) Halkier, A.; Helgaker, T.; Jørgensen, P.; Klopper, W.; Koch, H.; Olsen, J.; Wilson, A. K. *Chem. Phys. Lett.* **1998**, *286*, 243−252.
(54) Řezáč, J.; Riley, K. E.; Hobza, P. *J. Chem. Theory Comput.* **2011**, *7*, 2427−2438.
(55) Řezáč, J.; Riley, K. E.; Hobza, P. *J. Chem. Theory Comput.* **2011**, *7*, 3466−3470.
(56) Řezáč, J.; Hobza, P. *J. Chem. Theory Comput.* **2013**, *9*, 2151−2155.
(57) Boys, S.; Bernardi, F. *Mol. Phys.* **1970**, *19*, 553−566.
(58) *TURBOMOLE* V6.4 2012, a development of University of Karlsruhe and Forschungszentrum Karlsruhe GmbH, 1989−2007, TURBOMOLE GmbH, since 2007. Available from http://www.turbomole.com (accessed May 21, 2015).
(59) Weigend, F.; Häser, M.; Patzelt, H.; Ahlrichs, R. *Chem. Phys. Lett.* **1998**, *294*, 143−152.
(60) Podeszwa, R.; Szalewicz, K. *J. Chem. Phys.* **2007**, *126*, 194101.
(61) Sebetci, A.; Beran, G. J. O. *J. Chem. Theory Comput.* **2010**, *6*, 155−167.
(62) Stone, A. J.; Misquitta, A. J. *Int. Rev. Phys. Chem.* **2007**, *26*, 193−222.
(63) Misquitta, A. J.; Stone, A. J. *Mol. Phys.* **2008**, *106*, 1631−1643.
(64) Wen, S.; Beran, G. J. O. *Cryst. Growth Des.* **2012**, *12*, 2169−2172.
(65) von Lilienfeld, O. A.; Tkatchenko, A. *J. Chem. Phys.* **2010**, *132*, 234109.
(66) DePrince, A. E.; Sherrill, C. D. *J. Chem. Theory Comput.* **2013**, *9*, 293−299.
(67) DePrince, A. E.; Sherrill, C. D. *J. Chem. Theory Comput.* **2013**, *9*, 2687−2696.

DOI: 10.1021/acs.jctc.5b00281
J. Chem. Theory Comput. XXXX, XXX, XXX−XXX

(68) Turney, J. M.; Simmonett, A. C.; Parrish, R. M.; Hohenstein, E. G.; Evangelista, F. A.; Fermann, J. T.; Mintz, B. J.; Burns, L. A.; Wilke, J. J.; Abrams, M. L.; Russ, N. J.; Leininger, M. L.; Janssen, C. L.; Seidl, E. T.; Allen, W. D.; Schaefer, H. F.; King, R. A.; Valeev, E. F.; Sherrill, C. D.; Crawford, T. D. *WIREs: Comput. Mol. Sci.* **2012**, *2*, 556−565.
(69) Grimme, S.; Ehrlich, S.; Goerigk, L. *J. Comput. Chem.* **2011**, *32*, 1456−1465.
(70) Neese, F. *Wiley Interdiscip. Rev.: Comput. Mol. Sci.* **2012**, *2*, 73−78.
(71) Werner, H.-J.; Knowles, P. J.; Knizia, G.; Manby, F. R.; Schütz, M.; Celani, P.; Korona, T.; Lindh, R.; Mitrushenkov, A.; Rauhut, G.; Shamasundar, K. R.; Adler, T. B.; Amos, R. D.; Bernhardsson, A.; Berning, A.; Cooper, D. L.; Deegan, M. J. O.; Dobbyn, A. J.; Eckert, F.; Goll, E.; Hampel, C.; Hesselmann, A.; Hetzer, G.; Hrenar, T.; Jansen, G.; Köppl, C.; Liu, Y.; Lloyd, A. W.; Mata, R. A.; May, A. J.; McNicholas, S. J.; Meyer, W.; Mura, M. E.; Nicklass, A.; O'Neill, D. P.; Palmieri, P.; Peng, D.; Pflüger, K.; Pitzer, R.; Reiher, M.; Shiozaki, T.; Stoll, H.; Stone, A. J.; Tarroni, R.; Thorsteinsson, T.; Wang, M. *MOLPRO*, version 2012.1, a package of ab initio programs. See http://www.molpro.net (accessed May 21, 2015).
(72) Werner, H.-J.; Knowles, P. J.; Knizia, G.; Manby, F. R.; Schütz, M. *Wiley Interdiscip. Rev.: Comput. Mol. Sci.* **2012**, *2*, 242−253.
(73) Řezáč, J.; Jurečka, P.; Riley, K. E.; Černý, J.; Valdes, H.; Pluháčková, K.; Berka, K.; Řezáč, T.; Pitoňák, M.; Vondrášek, J.; Hobza, P. *Collect. Czech. Chem. Commun.* **2008**, *73*, 1261−1270.
(74) BEGDB. http://www.begdb.com/ (accessed May 21, 2015).
(75) Cybulski, S. M.; Lytle, M. L. *J. Chem. Phys.* **2007**, *127*, 141102.
(76) Gerenkamp, M.; Grimme, S. *Chem. Phys. Lett.* **2004**, *392*, 229−235.
(77) Distasio, R. A.; Head-Gordon, M. *Mol. Phys.* **2007**, *105*, 1073−1083.
(78) Hill, J. G.; Platts, J. A. *J. Chem. Theory Comput.* **2007**, *3*, 80.
(79) Chalasinski, G.; Szczesniak, M. M.; Cybulski, S. M. *J. Chem. Phys.* **1990**, *92*, 2481−2487.
(80) Lotrich, V. F.; Szalewicz, K. *J. Chem. Phys.* **1997**, *106*, 9688−9702.
(81) Weigend, F.; Ahlrichs, R. *Phys. Chem. Chem. Phys.* **2005**, *7*, 3297−3305.
(82) Goerigk, L.; Kruse, H.; Grimme, S. *ChemPhysChem* **2011**, *12*, 3421−3433.
(83) Cohen, A. J.; Mori-Sánchez, P.; Yang, W. *Science* **2008**, *321*, 792−794.
(84) Cohen, A. J.; Mori-Sanchez, P.; Yang, W. *Chem. Rev.* **2012**, *112*, 289−320.
(85) Tkatchenko, A.; von Lilienfeld, O. *Phys. Rev. B* **2008**, *78*, 045116.
(86) Otero-de-la Roza, A.; Johnson, E. R.; DiLabio, G. A. *J. Chem. Theory Comput.* **2014**, *10*, 5436−5447.
(87) Bader, R. F. W.; Stephens, M. E. *J. Am. Chem. Soc.* **1975**, *97*, 7391−7399.
(88) Fradera, X.; Austen, M. A.; Bader, R. F. W. *J. Phys. Chem. A* **1999**, *103*, 304−314.
(89) Fradera, X.; Poater, J.; Simon, S.; Duran, M.; Sola, M. *Theor. Chem. Acc.* **2002**, *108*, 214−224.
(90) Keith, T. A. *AIMAll* (Version 14.11.23); TK Gristmill Software: Overland Park, KS, USA, 2014. aim.tkgristmill.com (accessed May 21, 2015).
(91) Kannemann, F. O.; Becke, A. D. *J. Chem. Theory Comput.* **2009**, *5*, 719−727.
(92) Gillan, M. J. *J. Chem. Phys.* **2014**, *141*, 224106.

DOI: 10.1021/acs.jctc.5b00281
J. Chem. Theory Comput. XXXX, XXX, XXX−XXX